

# Metallicity effects on the Cepheid extragalactic distance scale from EROS photometry in the Large Magellanic Cloud and the Small Magellanic Cloud<sup>\*</sup>

D.D. Sasselov<sup>1,2</sup>, J.P. Beaulieu<sup>2</sup>, C. Renault<sup>3</sup>, P. Grison<sup>2</sup>, R. Ferlet<sup>2</sup>, A. Vidal-Madjar<sup>2</sup>, E. Maurice<sup>5</sup>, L. Prévot<sup>5</sup>, E. Aubourg<sup>3</sup>, P. Bareyre<sup>3</sup>, S. Brehin<sup>3</sup>, C. Coutures<sup>3</sup>, N. Delabrouille<sup>3</sup>, J. de Kat<sup>3</sup>, M. Gros<sup>3</sup>, B. Laurent<sup>3</sup>, M. Lachièze-Rey<sup>3</sup>, E. Lesquoy<sup>3</sup>, C. Magneville<sup>3</sup>, A. Milsztajn<sup>3</sup>, L. Moscoso<sup>3</sup>, F. Queinnec<sup>3</sup>, J. Rich<sup>3</sup>, M. Spiro<sup>3</sup>, L. Vigroux<sup>3</sup>, S. Zylberajch<sup>3</sup>, R. Ansari<sup>4</sup>, F. Cavalier<sup>4</sup>, M. Moniez<sup>4</sup>, C. Gry<sup>6</sup>, J. Guibert<sup>7</sup>, O. Moreau<sup>7</sup>, and F. Tajhmady<sup>7</sup>

<sup>1</sup> Harvard-Smithsonian Center for Astrophysics, 60 Garden St., MA 02138, Cambridge, USA

<sup>2</sup> Institut d'Astrophysique de Paris CNRS, 98bis boulevard Arago, F-74014 Paris France

<sup>3</sup> CEA, DSM/DAPNIA, Centre d'études de Saclay, F-91191 Gif-sur-Yvette, France

<sup>4</sup> Laboratoire de l'Accélérateur Linéaire IN2P3, Centre d'Orsay, F-91405 Orsay, France

<sup>5</sup> Observatoire de Marseille, 2 place Le Verrier, F-13248 Marseille 04, France

<sup>6</sup> Laboratoire d'Astronomie Spatiale CNRS, Traversée du siphon, les trois lucs, F-13120 Marseille, France

<sup>7</sup> Centre d'Analyse des Images de l'Institut National des Sciences de l'Univers, CNRS Observatoire de Paris, 61 Avenue de l'Observatoire, F-75014 Paris, France

Received 12 November 1996 / Accepted 13 February 1997

**Abstract.** This is an investigation of the period-luminosity relation of classical Cepheids in samples of different metallicity. It is based on 481 Cepheids in the Large and Small Magellanic Clouds from the blue and red filter CCD observations (most similar to  $V_J$  &  $R_J$ ) of the French EROS microlensing project. The data-set is complete and provides an excellent basis for a differential analysis between LMC and SMC. In comparison to previous studies of effects on the PL-relation, the EROS data-set offers extremely well-sampled light curves and well-filled instability strips. This allows reliable separation of Cepheids pulsating in the fundamental and the first overtone mode and derivation of differential reddening.

Our main result concerns the determination of distances to galaxies which are inferred by using the LMC as a base and using two color photometry to establish the amount of reddening. We find a zero-point offset between SMC and LMC which amounts to a difference between inferred and true distance modulus of  $0.14 \pm 0.06$  mag in the  $VI_c$  system. The offset is exactly the same in both sets of PL-relations – of the fundamental and of the first overtone mode Cepheids. No effect is seen on the slopes of the PL-relations, although the fundamental and the first overtone mode Cepheids have different PL slopes. We attribute the color and the zero-point offset to the difference in metallicity between the SMC and LMC Cepheids. A metallicity effect of that small magnitude still has important consequences

for the inferred Cepheid distances and the determination of  $H_0$ . When applied to recent estimates based on *HST* Cepheid observations, our metallicity dependence makes the low- $H_0$  values (Sandage et al. 1994) *higher* and the high- $H_0$  values (Freedman et al. 1994b) *lower*, thus bringing those discrepant estimates into agreement near  $H_0 \sim 70 \text{ km.s}^{-1} \text{ Mpc}^{-1}$ .

**Key words:** stars: Cepheids – distance – stars: abundances

---

## 1. Introduction

The Cepheid period-luminosity (PL) relation is widely accepted as being one of the most accurate primary distance indicators to nearby galaxies. It has now been applied as far as the Virgo cluster of galaxies (Freedman et al. 1994b, Pierce et al. 1994, Sandage et al. 1994, Tanvir et al. 1995) and holds the greatest promise to settle the debate over the value of the Hubble constant by providing a  $\pm 10\%$  accurate determination (the goal of the *HST* Key Project).

The Cepheid variable stars offer a simple way of measuring distances: their pulsation periods (easy to obtain) are strongly correlated with their luminosities; then distances are determined from their apparent brightness via the PL relation. The reliability of these distances stems from the good theoretical understanding of the Cepheids and their PL relation (Iben & Tuggle 1975). Theory predicts a small, but not negligible, abundance effect

Send offprint requests to: D. Sasselov (USA address)

<sup>\*</sup> This work is based on observations at the European Southern Observatory, La Silla, Chile.

on the PL zero point (see Stothers 1988 for review). However the ambiguous results of previous empirical tests for this effect have led all recent *HST* studies quoted above to assume that the Cepheid PL relation is insensitive to metallicity.

Three sources contribute to an abundance dependence of the PL relation: (1) theory of stellar pulsation, through the dependence of period on mass and radius; (2) theory of stellar evolution, through the mass-luminosity relation; and (3) theory of stellar atmospheres, through line blanketing and backwarming, *i.e.* the relations between effective temperature, absolute magnitudes in bandpasses, and bolometric correction. As a result, a metal-poor Cepheid is always fainter than a metal-rich Cepheid (at a fixed period and temperature); metal-poor Cepheids are also hotter (bluer) on the average. Given the sensitivity of each of the above three sources to metallicity, the overall weakness of the effect on the bolometric PL relation is remarkable (Stothers 1988, Chiosi et al. 1993). Theory predicts that the slope of the PL relation is nearly independent of metallicity, only the zero point is affected. The observed PL relations are not bolometric, hence the effect would depend on the bandpass. Most of the above predictions are valid for a limited range of Cepheid pulsation periods – Cepheids with  $P \geq 50$  days are expected (and observed) to deviate from a linear PL relation.

Theory in itself predicts a period-luminosity-color relation (Sandage 1958). However we study the PL relation, because this is the current one of choice in the determination of  $H_0$ . Theory predicts abundance effects on the PL relation due to helium (Y) and heavy elements (Z). However we only know the heavy elements abundances (Z) in Magellanic Clouds Cepheids, hence we speak of metallicity effects in this paper.

Previous studies have looked for metallicity effects on the Cepheid PL relation since the beginning of the 70s, but the issue remains unsettled observationally. Partly to blame is the near degeneracy between three important observed properties of Cepheids: the lines of constant period, reddening, and metallicity, in optical and near-infrared bandpasses. The lines of constant period represent the range of temperatures over which a star can sustain a stable Cepheid pulsation in a given mode and period; this introduces a natural width (in luminosity) to the PL relation. The amount of obscuration (reddening) is a more serious problem, as it is common practice to derive it from the photometry of the Cepheids themselves – thus the color difference due to metallicity will affect the reddening estimate and the inferred distance (Stothers 1988, Freedman & Madore 1990).

The first large scale comparison between SMC, LMC, and Galaxy Cepheids is due to Payne-Gaposchkin & Gaposchkin (1973). Payne-Gaposchkin (1974) concluded that there was no evidence for composition differences. However, Gascoigne (1974) reinvestigated the apparent color differences between LMC and SMC Cepheids as a metallicity effect and found that the SMC Cepheids would be fainter than LMC Cepheids by 0.1 mag (in  $V$ ). The color shift between LMC and SMC Cepheids was confirmed by Martin, Warren, & Feast (1979) and clearly distinguished from differential extinction. Subsequently, Iben & Tuggle (1975) and Iben & Renzini (1984) argued for a much smaller effect, mostly from theoretical considerations.

Stothers (1988) offered a critical review of all these attempts and pointed out the effect of the reddening correction. In a different approach to the problem, Caldwell & Coulson (1985, 1986) merged theoretical and empirical relations and individual reddenings from color-color diagrams to derive PL relations *adjusted* for abundance differences. These fit well their data-set of about 130 Cepheids in LMC and SMC. Caldwell & Coulson's results confirm the existence of a metallicity effect. Their very different approach provides no base for a detailed comparison with the current extragalactic use (Stothers 1988, Madore & Freedman 1991). In addition, Caldwell & Coulson's sample of about 130 Cepheids appears to be too small for quantifying the tiny effect. This can be seen in a recent comparison of primary distance indicators to 15 galactic and extragalactic objects in which Caldwell & Coulson's PL relations (*adjusted* for metallicity) were used (Huterer, Sasselov, & Schechter 1995) – the uncertainties within and between the four primary indicators are larger than the weak metallicity dependence.

The main reason extragalactic distance measurements have assumed that Cepheid luminosity does not depend on metallicity is the work by Freedman & Madore (1990). They found that any distance differences in three M 31 fields with varying metallicity are consistent with statistical noise, and much smaller than Stothers' (1988) prediction. The conclusion is based on a sample of 38 Cepheids and 152 *BVRI* observations; the method used is the same used in all recent distance determinations. The situation was reviewed by Feast (1991), who urged for the need to test the metallicity corrections empirically. This was partially accomplished by Laney & Stobie (1994), who concluded that their *VJHK* data on 21 Galactic and 115 MC Cepheids do not support the implications of Freedman & Madore's result that intrinsic Cepheid color is independent of metallicity. At the same time Gould (1994) challenged Freedman & Madore's conclusion by pointing out the high degree of correlation among the *BVRI* measurements (treated by Freedman & Madore as independent). Gould obtained a PL zero-point shift similar to that of Stothers (1988) by reanalyzing the same *BVRI* observations of 36 Cepheids in M 31. However, he showed that the data-set suffers from some systematic uncertainty, which affects the derived size of the effect. Stif (1995) confirmed independently Gould's conclusions using current theoretical evolutionary and atmosphere models. Thus the issue remained unsettled. As a result all recent HST measurements of Cepheid distances assume that no metallicity effects are present at V and I (Freedman et al. 1994b, Sandage et al. 1994, Tanvir et al. 1995).

In this paper we use a new data-set of two-color photometry ( $\sim 3$  million observations) of about 500 Cepheids in the LMC and SMC to derive the dependence of the optical PL relations on metallicity. We find that the apparent distance modulus depends on metallicity roughly as:  $0.4([Fe/H]+0.3)$ . The dependence is weaker than some previous claims, though by no means negligible. It is derived from a differential LMC-SMC analysis which incorporates all correlations between Cepheid measurements, independently derived metal abundances for Cepheids and supergiants, and known limits to the extinction laws. The photometric database is a byproduct of the EROS microlensing sur-

vey (Aubourg et al. 1993a, Beaulieu et al. 1995, Beaulieu et al. 1996).

## 2. The observations

The EROS (Expérience de Recherche d’Objets Sombres) French collaboration (Aubourg et al. 1993a, 1993b, 1995), and the MACHO project (Alcock et al. 1993) are both searching for baryonic dark matter in the galactic halo through microlensing effects on stars of the Magellanic Clouds. The EROS CCD equipment has been described by Arnaud et al. (1994). The observation, reduction, and calibration procedures have been described by Grison et al. (1995). All details on the Cepheids discovered and analyzed in the LMC and SMC are given in Beaulieu et al. (1995) and Beaulieu et al. (1996), respectively.

In brief, all observations were obtained at ESO, La Silla using a 0.4-m,  $f/10$  reflector and a  $2 \times 8$  mosaic of 16 CCDs. Two broad-band filters were used –  $B_E$  and  $R_E$ , with central wavelengths which fall roughly between Johnson  $B$  and  $V$  and  $R$  and  $I$ , respectively. The observations were obtained during the 1991-92 and 1993-95 seasons.

Our differential analysis relies on no external zero-point, and is thus completed within the  $B_E, R_E$  system. However, in applying our metallicity effect to the  $VI$  work with the HST, we have investigated our transformation between  $B_E, R_E$  and  $V, I$ . The net transmission of the  $B_E$  band is affected by the blue cutoff of the CCDs sensitivity, and is thus much closer to Johnson  $V$  than to  $B$ . The  $R_E$  bandpass remains intermediate between Cousins  $R$  and  $I$ . The  $B_E$  filter is broader than Johnson  $V$  in a similar way as the  $HST$  F555W filter is broader than  $V$ . The  $V - I$  and  $B_E - R_E$  colors transform well between each other as a result:  $V - I = 1.02(B_{E2} - R_{E2})$ ,  $\sigma = 0.02 \text{ mags}$ . The LMC data from the 1991-92 season was obtained with somewhat different set of blue-red filters. Therefore we treated the LMC Cepheid data as two different sets and compared each of them separately to the SMC data. The 1991-92 season LMC data is useful because of the large number of observations. With thousands of stars available in the Cepheids range of magnitudes and colors on the EROS CCD frames, constructing an accurate and reliable photometric transformation is easy. We transformed all old  $B_{E1}, R_{E1}$  photometry to the new  $B_{E2}, R_{E2}$  system by:

$$B_{E2} - B_{E1} = -0.680 \pm 0.060 - 0.175 \pm 0.005(B_{E1} - R_{E1}),$$

$$R_{E2} - R_{E1} = -0.116 \pm 0.060 - 0.100 \pm 0.005(B_{E1} - R_{E1})$$

The two sets of LMC data are very similar and produced the same result in the final differential analysis.

The identification of Cepheids in both Clouds is based on the Fourier components of their light curves and mean magnitudes in the expected luminosity range. Several Cepheids were excluded from our analysis on the basis of strong blending. These could be either actual physical binaries, or unresolved stars along the line of sight. They are easy to identify by the form of the pulsation loop on the color-magnitude diagram (Fig. 1) and by the accompanying deviation of their mean magnitude

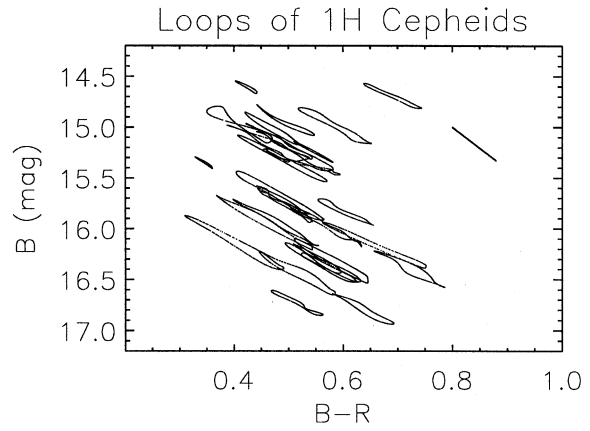


**Fig. 1.** The loops which Cepheids complete during a pulsation cycle in the temperature-luminosity plane. The form of a loop reflects the thermodynamic relation between stellar radius and temperature change, plus a small nonlinear effect on the emergent radiation due to the Cepheid atmosphere. Whenever a constant flux is added to that of the Cepheid, the loop looks like an “eight” (a bluer blend) or has a “hysteresis”-like form (a redder blend). One of each examples are shown on this figure of first overtone LMC Cepheids – in the upper left and lower right sides of the instability strip, respectively.

and color from the rest of the Cepheid sample. Examining the pulsation loops shows that background blending for the LMC and SMC Cepheids is not a problem (affects less than 10% of them), as should be expected for luminous stars like them. We investigated several possible sources of difference between the LMC and SMC photometry, like airmass and the Pinatubo eruption, but found their effect to be insignificant.

## 3. The concept

The concept is simple - we have two complete Cepheid samples with known difference in metallicity  $\Delta[Fe/H]_{LMC-SMC} = 0.35$  (Spite & Spite 1991; Luck & Lambert 1992). This is an average difference between spectroscopic abundances of longer-period Cepheids. We compare the two samples in the period-magnitude-color (PLC) manifold to derive 2 independent sources of difference – distance and extinction, and to search for a *third* source – metallicity.

For each Cepheid we have 3 observed quantities: two coordinates and a pulsation period; and 2 observed data-sets: complete light curves in  $B_E$  and  $R_E$ . The 2 data-sets (light curves) give two observed quantities: the time-averaged, intensity-weighted mean magnitudes; thus each Cepheid has 5 observed quantities in total. The light curves also provide independently the means to separate Cepheids of different pulsation modes and to treat background blending.

We construct the PL relations in each band,  $B_E, R_E$ , of LMC and SMC Cepheids, *i.e.* the observed mean magnitudes,  $Q_{i,k}$ , for each Cepheid of period  $P_k$  and each band,  $i$ , are fit to a linear function:

$$Q_{i,k} \sim \alpha_i + \beta_i \log P_k, \quad (1)$$

where  $\alpha_i$  are the zero points and  $\beta_i$  are the slopes; within our completeness –  $P \leq 30$ days, the PL relations are found to be linear. We compare the two Cepheid sets in the PL plane. They are offset in luminosity ( $Q_i$ ) due to two sources: difference in distance between LMC and SMC, and difference in extinction towards LMC and SMC. We search for a *third* source – a term due to the difference in metallicity.

Two PL relations (PL- $B_E$  and PL- $R_E$ ) in each of the Clouds can give us the distance difference and the reddening difference, but the metallicity effect remains degenerate. We search to lift this degeneracy by going to the period-magnitude-color (PLC) space, and imposing constraints on the interstellar extinction. We fix the mean reddening in LMC as  $E(B-V)=0.10$ , the value adopted by all *HST* teams, and we adopt independent estimates for the foreground reddenings to LMC and SMC. Now, given a large observed sample (in a statistical sense), we can compare differentially the PLC distributions of LMC and SMC Cepheids. Such a comparison will constitute a fit to a multi-parameter model. Two of the model parameters are metallicity terms.

We chose as our goal to evaluate the metallicity effects on the LMC-based technique used by all *HST* teams (*e.g.* Madore & Freedman 1991; hereafter – the modern technique) for two reasons. First, the current Cepheid-based  $H_0$  is exclusively derived by it. Second, the EROS Cepheid sample provides an excellent opportunity to accomplish that goal, being obtained with two filters ( $B_E, R_E$ ) similar to the *HST* F555W, F814W filters, and being LMC-based too.

We emphasize the need to account for the correlations between magnitude measurements, which has not been done in its applications to-date. This rigorous approach was pioneered by Gould (1994); our analysis draws heavily on it and expands it. Due to the strong correlations and near-degeneracies present in the problem, we see no alternative to the rigorous approach.

Hereafter the notation  $\delta x$  will refer to the metallicity dependence of the quantity  $x$  in the sense:  $\Delta x_{\text{inferred}} + \delta x = \Delta x_{\text{true}}$ , where  $\Delta x = x_{SMC} - x_{LMC}$ .

#### 4. The method

Our method applies the same basic techniques for modeling of data (Press et al. 1994, Sect. 15) introduced earlier by Gould (1994), but deviates substantially from Gould's analysis. The difference is that we solve for a metallicity effect which is a function of bandpass/wavelength. Therefore we model our data in the three-dimensional PLC manifold, as opposed to just the PL plane. Thus our analysis follows the current state of theoretical understanding (Stothers 1988; Chiosi et al. 1993; Stiff 1995), and takes advantage of the fact that our SMC data-set fills densely the PLC manifold.

Here we present a simultaneous fit of the LMC and SMC data. The two ( $B_E, R_E$ ) magnitude measurements of each Cepheid are treated as correlated with each other, but not with

the measurements of any other Cepheid. Then we can write the  $\chi^2$  merit function as

$$\chi^2 = \sum_{n=1}^4 \sum_{k=1}^{N(n)} \sum_{i,j=1}^2 b_{ij}^n X_{i,k}^n X_{j,k}^n \quad (2)$$

where  $n = 1, 2$  correspond to the LMC data (with  $N(n)$  Cepheids) on the period-magnitude and color-magnitude planes, respectively;  $n = 3, 4$  correspond similarly to the SMC data (with  $N(n)$  Cepheids);  $i = 1, 2$  are the two bandpasses ( $B_E, R_E$ ), and where the residuals are defined as follows:

$$X_{i,k}^1 = Q_{i,k} - (\alpha_i + \beta_i \log P_k), \quad (3)$$

$$X_{i,k}^2 = Q_{i,k} - [a_i + b_i(Q_{1,k} - Q_{2,k})], \quad (4)$$

$$X_{i,p}^3 = Q_{i,p} - (\alpha_i + \beta_i \log P_p + \gamma_1 + \gamma_2 R_i + \gamma_3^i), \quad (5)$$

$$X_{i,p}^4 = Q_{i,p} - [a_i + b_i(Q_{1,p} - Q_{2,p} + \gamma_2(R_2 - R_1) + \gamma_3^1 - \gamma_3^2) + \gamma_1 + \gamma_2 R_i + \gamma_3^i], \quad (6)$$

with  $k, p = 1, \dots, N(n)$  being the number of Cepheids in LMC and SMC, respectively. The covariance matrices of the data are then

$$c_{ij}^n = \frac{1}{N(n) - 1} \sum_{k=1}^{N(n)} X_{i,k}^n X_{j,k}^n \quad (7)$$

for  $n = 1, 2$ , and

$$c_{ij}^n = \frac{1}{N(n) - 1} \sum_{p=1}^{N(n)} (X_{i,p}^n - \overline{X_i^n})(X_{j,p}^n - \overline{X_j^n}) \quad (8)$$

for  $n = 3, 4$ , where

$$\overline{X_i^n} = \frac{1}{N(n)} \sum_{p=1}^{N(n)} X_{i,p}^n. \quad (9)$$

In Eq. (2),  $b_{ij}$  is the inverse covariance matrix of the data,  $b = c^{-1}$ .

The above set of equations illustrates our differential analysis of LMC and SMC Cepheids as *ensembles* of stars. Each Cepheid with a period  $P_k$ , and mean magnitudes  $Q_{i,k}$  is fitted (for each band) to a linear function of the period – the PL relation ( $\alpha_i, \beta_i$ ), and to the instability strip ( $a_i, b_i$ ). Thus, for the LMC Cepheids we have the residuals in Eqs. (3) and (4). The residuals of the SMC Cepheids will contain four additional linear terms: (1) one due to the distance difference ( $\gamma_1 = \mu_{SMC} - \mu_{LMC}$ ); (2) one due to extinction – the relative reddening  $\gamma_2 = \Delta E(B - V)$ , and  $R_i$  being the adopted reddening vector (see Sect. 6 below); and (3) two (one for each band) due to metallicity difference ( $\gamma_3^i$ ). All of these terms simply add on to the zero point of the PL relation (for each band), and that is what Eq. (5) is all about.

The SMC residuals from Eq. (6) have a slight complication, which will become clear here. Let  $M_i$  ( $i = 1, 2$ ) be the absolute magnitudes in  $B_E$  and  $R_E$ , respectively. They define the PL relations for each band:  $M_i(PL) = \alpha_i + \beta_i \log P$ . Then following the metallicity term,  $\gamma_3$ , introduced above, the resulting changes in  $M_i$  are simply:  $\delta M_1 = \gamma_3^1$  and  $\delta M_2 = \gamma_3^2$ . Color is defined as:  $(Q_1 - Q_2)_0 = M_1 - M_2$ , where the subscript “0” means corrected for extinction; hence the color change at a fixed period due to the metallicity difference between LMC and SMC will be:

$$\delta(Q_1 - Q_2)_0 = (\gamma_3^1 - \gamma_3^2). \quad (10)$$

This term,  $\gamma_3^1 - \gamma_3^2$ , will appear in the period-color plane together with the reddening ( $\gamma_2$ )-term alone. The equation of the linear period-color relation is not added to Eqs. (3)-(6) to minimize redundancy; its slope will be simply  $(\beta_1 - \beta_2)$ .

Now we can describe the meaning of Eq. (6) and the residuals in the color-magnitude plane. In the color-magnitude plane we have the more complex case, where both the color and the magnitude are affected by both the reddening *and* the metallicity. While the terms for the magnitude remain the same as in Eq. (5), the terms for the color will come from Eq. (10) for the metallicity, and from the definition of extinction color correction. The latter definition is:  $(Q_1 - Q_2)_0 = (Q_1 - A_1) - (Q_2 - A_2)$ , where the  $A_i$  are the total extinctions in each band,  $A_i = E_{B-V} R_i$ ; hence  $(Q_1 - Q_2)_0 = (Q_1 - Q_2) - E_{B-V}(R_1 - R_2)$ . Thus Eq. (6) describes the following aspect of our model: more extinction makes Cepheids redder and fainter. As far as the metallicity terms are concerned, they are not constrained (although theory predicts that more metals make Cepheids redder and brighter). We constrain the reddening term by not allowing unphysical negative values, and further by considering the foreground extinction towards the SMC as its lower limit (see Sects. 5 and 6).

To obtain the true distance modulus  $(m - M)_0 \equiv \mu$ , the observed mean magnitude must be first corrected for extinction:  $\mu = (Q_1 - A_1) - M_1 = (Q_2 - A_2) - M_2$ . If  $A_i$  are derived from the observations of the Cepheids themselves, the metallicity dependence of the true distance modulus will be a combination of the dependencies of the absolute magnitudes and the color (Stothers 1988). Using the standard definitions for the ratio of total to selective extinction, we have:  $R_i = A_i / E_{B-V} = (R_1 - R_2) A_i / E_{Q_1 - Q_2}$ , where  $E_{Q_1 - Q_2} = (Q_1 - Q_2) - (Q_1 - Q_2)_0$ . Keeping  $R_i$  fixed, we obtain for the change of distance modulus with metallicity:

$$\begin{aligned} \delta\mu &= -\delta M_i + \frac{R_i}{R_1 - R_2} \delta(Q_1 - Q_2)_0 = \\ &= -\gamma_3^i + (\gamma_3^1 - \gamma_3^2) \frac{R_i}{R_1 - R_2}, \end{aligned} \quad (11)$$

which applies to the use of a PL relation and is in units of stellar magnitude per  $\Delta Z$  of metals by mass. Stothers (1988) used this case (when  $A_i$  are derived from the Cepheids themselves) to derive the prototype of Eq. (11) from theoretical considerations. We follow the same case (referred to as the modern technique),

but derive the correction,  $\delta\mu$ , empirically from the differential analysis of the magnitudes, colors, and periods of LMC and SMC Cepheids. Therefore the application of our method (see next section) is restricted to this specific case. We derive the metallicity correction as  $\delta\mu = \Delta\mu_{\text{true}} - \Delta\mu_{\text{inferred}}$ .

We want to emphasize again that our fit is in the PLC space for the sole purpose of finding the residual color difference between the LMC and SMC Cepheids; we are not interested in deriving or using a PLC relation. It is our way of lifting the degeneracy between the effects of reddening and metallicity in the PL planes in our differential analysis of LMC and SMC. Freedman & Madore (1990) used a different approach to break this degeneracy – by setting  $\gamma_1 = 0$ , *i.e.* by observing three fields at the same distance but different metallicity. They cannot use our method, because their data-set (36 Cepheids) is too small to fill densely the PLC space. In other words, in the language of  $\chi^2$  statistics, their number of data points (36) will be comparable to the number of model parameters.

## 5. The application

As described by Eqs. (3)-(6) of the previous section, our model of the LMC-SMC comparison has 12 model parameters. To solve for all 12 parameters we adopt the following external constraints: (1) mean LMC extinction  $E(B-V)=0.10$  as used by the HST teams; (2) foreground extinctions of 0.06 for LMC and 0.05 for SMC (Bessell 1991); (3) no depth dispersion in the EROS LMC sample; and (4) the line of nodes for SMC from Caldwell & Coulson (1986) to derive the EROS SMC sample depth dispersion. These constraints are discussed in the next two sections. Obviously, there is one more projection – on the period-color plane, which is not included in Eqs. (3)-(6), but is trivially derived from them. One estimates the model parameters by minimizing in a statistical sense the residuals, given independent constraints on some of the parameters. To find the best fit one differentiates  $\partial\chi^2/\partial A_l = 0$ , where  $A_l$  is the 12 element vector of model parameters:

$$A = (\alpha_i, \beta_i, a_i, b_i, \gamma_1, \gamma_2, \gamma_3^i) \quad (i = 1, 2). \quad (12)$$

The  $\chi^2$  merit function of Eq. (2) can be rewritten in a more explicit form for our multidimensional fit:

$$\begin{aligned} \chi^2 &= \sum_{n=1}^4 \sum_{k=1}^{N(n)} \sum_{i,j=1}^2 b_{ij}^n [Q_{i,k}^n - \sum_{l=1}^{12} A_l f_{i,l}^n(P_k, (Q_1 - Q_2)_k)] \\ &\quad \times [Q_{j,k}^n - \sum_{l=1}^{12} A_l f_{j,l}^n(P_k, (Q_1 - Q_2)_k)] \end{aligned} \quad (13)$$

The differentiation yields a matrix equation which can be solved for  $A_l$ :

$$A_l = \sum_{q=1}^{12} C_{lq} D_q, \quad (14)$$

where  $C_{lq}$  is the covariance matrix of the model parameters vector,

$$C^{-1} \equiv B = \sum_{n=1}^4 \sum_{k=1}^{N(n)} \sum_{i,j=1}^2 b_{ij}^n f_{i,k,l}^n f_{j,k,q}^n, \quad (15)$$

with  $f_{i,k,l}^n$  being the basis functions from Eq. (13), given explicitly in Eqs. (3)-(6); in a similar fashion, the vector  $D_q$  relates the basis functions to the mean magnitudes  $Q_{i,k}^n$ .

The procedure requires an iteration (see Gould 1994). First, we construct period-magnitude and color-magnitude relations for the Cepheids in the LMC and derive the eight parameters  $\alpha_i, \beta_i, a_i, b_i$  from linear fits to the data. These are then used to find the covariance matrices of the LMC data (Eq. 7). Next, we compute the covariance matrices of the SMC data and find the best-fit values. We found that the slopes of the PL relations do not differ (within the uncertainties) between LMC and SMC; we adopt two unique slopes (one for fundamental, one for first overtone Cepheids) for both LMC and SMC. At this point we derive  $\Delta\mu_{\text{inferred}}$ , by setting  $\gamma_3^1 = \gamma_3^2 = 0$ . Then we minimize the residuals along a given reddening vector  $R_V$  and additionally constraining  $\gamma_2$  so that SMC Cepheids have no unphysical extinctions (negative). This constraint is derived independently of the fit (see next section). We use the same form of the Galactic extinction law (Cardelli, Clayton, & Mathis 1989) for all samples. We iterate this procedure until the best-fit parameters agree with the trial parameters used to estimate the covariances. Note that the entire procedure is separately done for the fundamental mode and first overtone mode Cepheids, and thus we have a strong constraint on the final derived parameters, which are invariant to the type of Cepheids used to derive them.

For illustration, the covariance matrix of the LMC fundamental Cepheids (Eq. 7) is:

$$c_{ij}^1 = \begin{pmatrix} 0.048 & 0.041 \\ 0.041 & 0.037 \end{pmatrix} \quad (16)$$

and for the SMC fundamental Cepheids (Eq. 8):

$$c_{ij}^3 = \begin{pmatrix} 0.103 & 0.073 \\ 0.073 & 0.084 \end{pmatrix}. \quad (17)$$

The correlation coefficients are obviously very high, as also seen in Figs.5 & 6.

For Cepheids all at the same distance and selected only by magnitude the PL relation is subjected to bias, which can be avoided by using the inverse regression (Schechter 1980, Feast 1995). We do not expect strong magnitude bias in our samples, but used both direct and inverse regressions in our fits.

The method above contains as a subset the procedures which comprise the modern technique for determining Cepheid distances (Madore & Freedman 1991). Namely, one begins by constructing the PL relations in the LMC, then fitting the mean magnitudes of the SMC Cepheids to the LMC in each band, and deriving apparent distance moduli for each band. These distance moduli are then fitted to an extinction law

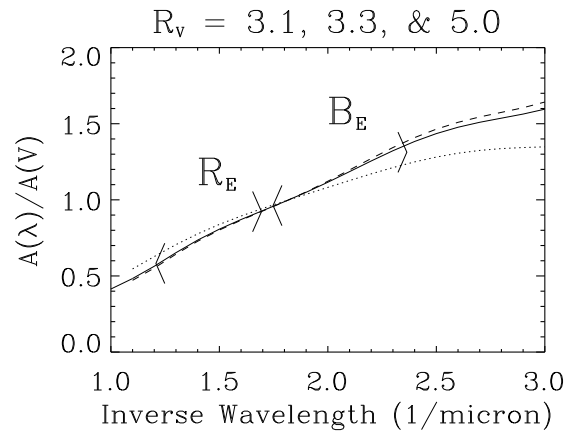


**Fig. 2.** The extinction diagram for three different extinction laws – with  $R_V=3.1$  (dashed),  $R_V=3.3$  (solid), and  $R_V=5.0$  (dotted). Here  $A(V)$  corresponds to the amount of extinction in the Johnson  $V$  band. The two EROS filters are marked on the diagram.

with an adopted parameter ( $R_V$ ) to derive the amount of reddening in the SMC data. Finally the reddening corrected, true distance modulus is determined. As brief as it is in this description, the technique overlooks several sources of physical scatter and systematics which could be present in the data. We study those below, since they are also part of our method to derive the metallicity dependence. They provide the independent constraints, which make possible the derivation of both  $\gamma_3^1$  and  $\gamma_3^2$ .

## 6. The extinction law and reddening

In our differential analysis between LMC and SMC the effect of interstellar reddening (and obscuration) is represented by the term  $\gamma_2 R_i$ , where  $\gamma_2 = \Delta E(B - V)$  and the reddening vector

$$R_i = (3.81, 2.48). \quad (18)$$

We use the  $R_V$ -dependent Galactic extinction law of Cardelli, Clayton, & Mathis (1989) and the above values correspond to a convolution of the EROS filters transmission curves with the  $R_V = 3.3$  extinction law (Fig. 2); here  $R_V = A(V)/E(B - V)$ . An extinction law with  $R_V = 3.3$  is widely accepted for the extinction in LMC (e.g. Freedman et al. 1994a), while for our Galaxy  $R_V = 3.1$  is more common on the average. There are a few lines-of-sight with  $R_V$  as high as 5.3, but that's very rare. Physically, high values of  $R_V$  appear to be related to systematically larger dust particles in dense regions. However, an empirical relation between the spectral “bump” at 2200 Å and  $R_V$  seems to lack physical grounds (Cardelli, Clayton, & Mathis 1989). When used, this relation predicts a high  $R_V$  value (as high as 5) for the SMC, where the 2200 Å feature is known to be very weak (Bessell 1991).

This is a good enough reason for us to investigate how our results are affected by the value of the extinction law parameter. Therefore we have convolved the transmission curves of the EROS filters with  $R_V = 3.1$  and  $R_V = 5.0$  extinction laws as well (Fig. 2). After deriving the apparent distance moduli

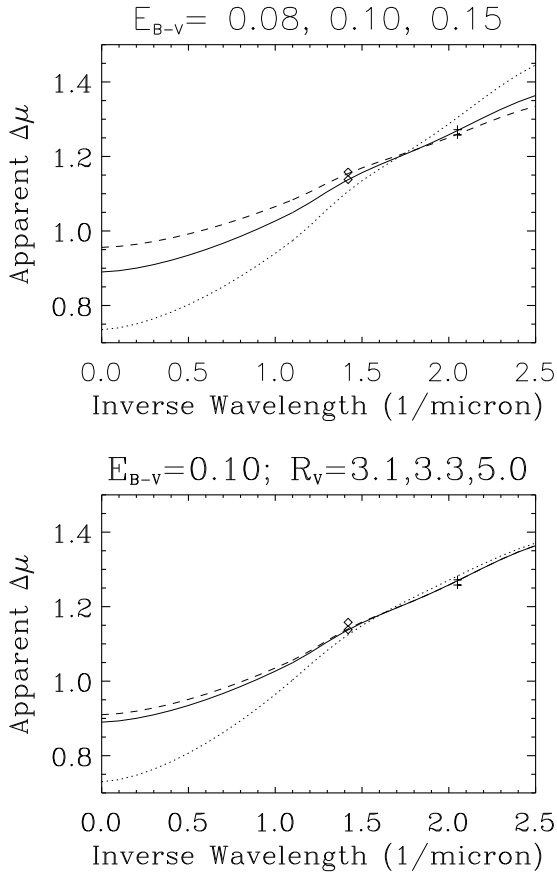


**Fig. 3a and b.** The differential apparent distance moduli for SMC Cepheids fitted with Galactic extinction laws: **a** for three different amounts of extinction, and **b** for three different reddening parameters,  $R_V$ . At each band we have two independent values for the distance moduli – for fundamental and first overtone Cepheids, respectively. The error bars on the values are as big as the symbols. No correction for metallicity effects has been applied at this point. The best fit for SMC is  $E(B-V)=0.09$  and  $R_V=3.3$ , but higher values of  $R_V$  are not excluded.

between SMC and LMC for each band *and* each mode of pulsation, we plot them against inverse wavelength at the effective centers of the photometric bands (Fig. 3). We fit through the points Galactic extinction laws with different amount of extinction, as measured by  $E(B-V)$ , and with different parameters,  $R_V$ .

Concerning the reddening of the Magellanic Clouds, it is important for our study to know the existing observational limits for the average values. First of all, we have the limit of foreground reddening. Towards the SMC the foreground (due mostly to our Galaxy) is smooth and  $E(B-V)$  lies between 0.04 and 0.06 mag (Bessell 1991). Within the SMC the reddening could vary between 0.06 and 0.3 mag. On the average the reddening of the LMC is very similar: foreground of 0.04 to 0.09, and same within (Bessell 1991). These values are derived independent of Cepheid observations and will prove very useful in our derivation of a metallicity dependence. Also, when we refer

to Cepheids in LMC and SMC, one should bear in mind that the Cepheid samples are located in the bar of LMC and near the central region of SMC. This is particularly important in terms of their mean reddenings (as samples); the central region of SMC is known to be dusty.

The extinction diagram in Fig. 3 provides an opportunity to derive individual reddenings for each Cepheid on our list, by fitting an extinction law with a fixed reddening parameter. The individual Cepheid reddenings are excellent for the study of the structure of the PL relation (see next section). In deriving individual reddenings we required that no Cepheid be assigned a reddening smaller than the known foreground reddening to the MC given above. As it will become clear from the next section, the so derived individual reddenings offer no additional advantage in the differential analysis.

It is well known that interstellar dust absorbs or scatters light in the optical range, hence extinction is by definition a non-negative quantity. In our estimate of the extinction,  $A_i$ , we need to bear this cutoff in mind, because  $A_i$  is small towards the LMC and SMC, and for a large subsample of our Cepheids we get negative values. Given the crucial use of the reddening cutoff in our analysis and final fit to the model, it is important to truncate the measurements of  $A_i$  properly, and preserve a useful estimate of the measurement uncertainty,  $\sigma_{A_i}$  in the process of doing so. The solution to finding the value of  $A_i$  and its error *together* with prior knowledge that  $A_i$  cannot be less than zero is given by Bayes's theorem. For an estimate of  $A_i$  with value  $x$  and normal error  $\sigma_x$ , and our knowledge of the distribution of the observed  $A_i$ ,  $p(A_i)$ , the probability distribution for the true  $A_i$  will be given by the Bayesian filter:

$$p(A_i | x, \sigma_x) = \frac{p(x | A_i, \sigma_x)p(A_i)}{p(x)} = \frac{p(A_i)e^{-\frac{(A_i-x)^2}{2\sigma_x^2}}}{\int_0^\infty p(A_i)e^{-\frac{(A_i-x)^2}{2\sigma_x^2}} dA_i}$$

A practical, and entirely satisfactory assumption would be that  $p(A_i)$  is a one-sided gaussian which has a maximum at  $A_i = 0$  and declines for large  $A_i$  (see Press 1996).

The conclusion of our analysis is that the reddening law in the bar of SMC is not very different from that of the LMC with a reddening parameter much closer to 3.3 than 5. Concerning the absolute value for the LMC reddening (currently used:  $E(B-V)=0.10$  and  $R_V=3.3$ ), our mean value, from the individual reddenings, is  $E(B-V)=0.10\pm 0.007$ . With the derived parameters in the next section we could constrain the mean reddening of the SMC Cepheids to  $E(B-V)\geq 0.10$ .

## 7. The PL relations - structure of the scatter

Now we are ready to apply our method. We start by constructing the PL relations (in each band) for the LMC and SMC Cepheids, separately for fundamental and first overtone pulsators (Fig. 4). All PL relations are essentially linear in the range of periods in our data. The slopes,  $\beta_i$  (Eq. 1), which are insensitive to moderate amounts of reddening, are the same in LMC and SMC:

$$\beta_1 = -2.78 \pm 0.16 \quad \text{and} \quad \beta_2 = -3.02 \pm 0.14 \quad \text{for fundamental mode}$$

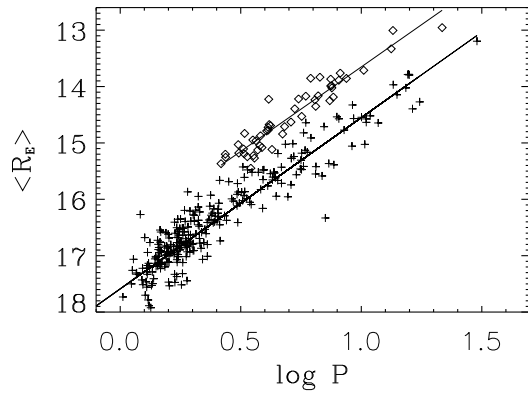


**Fig. 4.** The PL- $R_E$  relations for LMC and SMC Cepheids .

Cepheids in LMC, and

$\beta_1 = -2.72 \pm 0.07$  and  $\beta_2 = -2.96 \pm 0.06$  for SMC. Similarly, for the first overtone Cepheids we have:

$\beta_1 = -3.41 \pm 0.22$  and  $\beta_2 = -3.43 \pm 0.20$

for LMC, and  $\beta_1 = -3.46 \pm 0.14$  and  $\beta_2 = -3.52 \pm 0.13$  for SMC. This lack of metallicity dependence of the slopes, as well as the difference between  $\beta_1$  and  $\beta_2$  are in very good agreement with theory (Stothers 1988).

The scatter about the PL relations results from physical reasons, as well as statistical noise. On the basis of our very well sampled light curves in two bands, we have already excluded Cepheids which show evidence of blending, as well as stars which are not Cepheids, and can analyse the other physical sources of scatter.

Individually, each Cepheid in the LMC can be offset from the PL relation of the LMC Cepheids due to 3 independent sources: (1) position in the instability strip; (2) differential reddening within the LMC; (3) differential distance (depth) within the LMC. These three additional independent sources of scatter contribute to a natural width (in L) of the PL relation. They are manifested in the structure of the LMC covariance matrix (Eq. 7), where none of the sources lies in the plane defined by the other two sources; hence the covariance matrix would be three-dimensional. We illustrate this by plotting against each other the magnitude residuals defined in Eq. (3). In Fig. 5 we have the diagram of the residuals for the LMC fundamental Cepheids. The high level of correlation is evident. The diagram of the residuals shows that reddening (solid line) within the LMC is not the only source of scatter. In Fig. 6 we have the same diagram for the SMC Cepheids (Eq. 8); all of the above applies to them as well.

The diagrams of the residuals provide a nice illustration to the structure of the PL relations. For example, if the PL relation had no dispersion, all points would lie in the center (0,0) of the diagram (Fig. 5). Alternatively, if there were groupings of Cepheids separated in distance along the line of sight, they will appear clearly as clumps on the diagram.

If we deredden each Cepheid as described in the previous section Sect. 6, we are mostly left with the dispersion due to depth (Fig. 7). The reason is that the individual dereddening

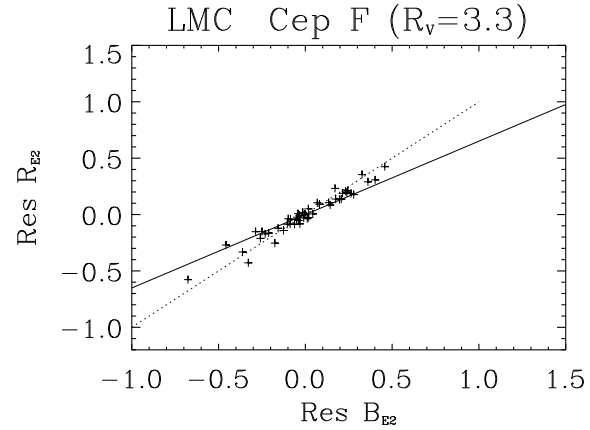


**Fig. 5.** The residuals in  $B_E$  and  $R_E$ , as defined in Eq. (3), plotted against each other for the fundamental Cepheids in LMC and their PL relations. The solid line is the reddening line for  $R_V=3.3$ . The line of constant periods is steeper. Dispersion due to distance is even steeper – along the diagonal (dotted line).

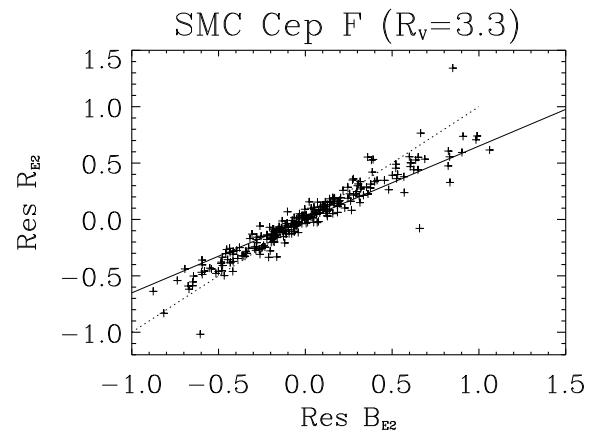


**Fig. 6.** The same as Fig. 5, but for the fundamental Cepheids in SMC. The solid line is the reddening line for  $R_V=3.3$ . The SMC Cepheids show a larger scatter, which is also closer to the diagonal line (due to distance dispersion).

corrects also for the width of the instability strip along the lines of constant period, at least partially. The correction is partial for two reasons: (1) the reddening and the  $P = const.$  lines are not completely degenerate (Fig. 8); and (2) the individual reddening is limited (from below) by the amount of foreground reddening (independently known).

The near-degeneracy of reddening and  $P = const.$  lines in the color-magnitude plane is worth investigating. We find that the slopes of the  $P = const.$  lines in LMC and SMC are practically the same:  $3.3 \pm 0.4$ ; while the slopes of reddening ( $B_E$ ) are 2.86 (for  $R_V=3.3$ ) and 3.53 (for  $R_V=5.0$ ). A limited illustration to this is given in Fig. 8; the Cepheids shown have been selected to have exactly the same periods (to the second digit) – in practice we use the whole data-set to derive the slopes.

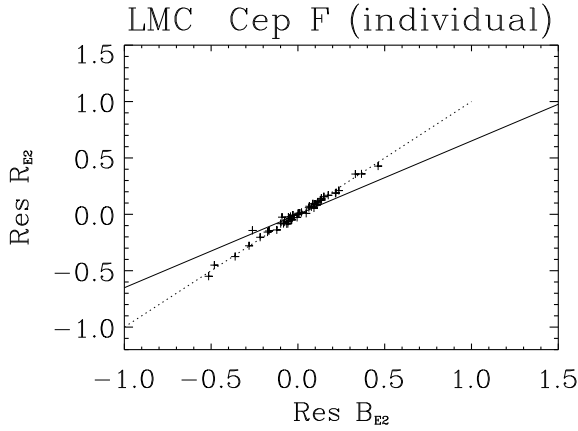


**Fig. 7.** The same as Fig. 5, except that each Cepheid has been dereddened individually using the Galactic extinction law with  $R_V=3.3$ . In comparison to Fig. 5, the dispersion has decreased and has shifted slope to the diagonal. All these Cepheids are in the bar of the LMC, which is face on, and that explains the very small depth dispersion we see. Conversely, in SMC we see a substantial depth (Fig. 6).

Now we turn to accounting for the depth of LMC and SMC. In this we employ for the first time the last two observed Cepheid quantities: the coordinates. We plot the magnitude residuals versus angle on the sky across the SMC ( $1^{\text{deg}}=0.0389$  mag) using the line of nodes for SMC from Caldwell & Coulson (1986). They derived them over areas which are about 25 times larger than the EROS CCD-array areas. The EROS areas cover only the LMC bar (which is seen face on) and the SMC bar (seen edge-on) and have dimensions of  $25' \times 71'$  on the sky. That is one reason we did not attempt our own derivation of the line of nodes of the Clouds. In deriving the depth dispersion in the SMC we used Cepheids along the line of nodes and orthogonal to it.

With the width of the instability strip derived from the color-magnitude plane to be  $\pm 0.22$  mags, we derive the depth dispersion in our SMC sample to be  $\pm 0.10$  mags. Our uncertainty in the value of  $R_V$  limits our ability to derive the internal amount of reddening within SMC to the ranges already known (Sect. 6). However, it provides a very valuable constraint from below on the overall reddening towards SMC as  $E(B-V) \geq 0.10 \pm 0.01$ ; otherwise half of the Cepheids will have negative extinctions, which is unphysical. We use this value to constrain  $\gamma_2$  in our multidimensional minimization (Eqs. 12-15).

Finally, we would like to point out that the EROS sample of SMC Cepheids happen to be mostly from the far arm and the main bar (see Figs.7&9 of Caldwell & Coulson 1986). Hence the sample is not likely to define the centroid of SMC well, and would result in a larger distance modulus difference with the LMC (by about  $0.15$  mags). This is of no consequence to our differential analysis here.

The diagrams of the residuals are independent of differential reddening or metallicity between the MCs, however understanding the structure of each PL relation and quantifying the sources of scatter improve the reliability of the differential anal-



**Fig. 8.** An excerpt of the Cepheid instability strip showing groups of Cepheids which happen to have the same periods – from top to bottom: 7.5, 5.5, 4.2, and 3.1 days, respectively. The open symbols correspond to LMC Cepheids, the rest – to SMC ones. The Cepheids shown have been dereddened as an ensemble in each MC, with  $R_V=3.3$ . The reddening lines for two values of  $R_V$  are shown in the lower left corner.

ysis. When we compare the LMC and SMC PL relations, the above three sources of scatter are not involved (as long as we have a statistically large sample of data points, *i.e.* Cepheids) – we use *ensemble* quantities. Then it is only consistent to use the “ensemble” reddening for each MC, the individual reddenings will introduce a bias. Other sources of scatter have been proposed in a critique of the PLC relation – mass loss and different strip crossings (Stift 1982, 1995). We do not identify another source in our data and in the remaining scatter; such effects must be subtle for the PL relation alone.

## 8. Results

### 8.1. The effect of metallicity

We apply the procedure in Sect. 5 to the data-sets of fundamental mode and first overtone mode Cepheids separately and obtain very similar results. There are enough first overtone Cepheids, 27 and 141 respectively, to make this result statistically significant. Thus, the two sets of PL relations give the same distance modulus difference (SMC-LMC) of  $0.86 \pm 0.045$  mag (before corrections for reddening and metallicity). This illustrates for the first time the usefulness of the PL relation of first overtone Cepheids for determining distances.

The model parameters derived from the fits of the different datasets are as follows:  $\alpha'_i, \beta_i = 17.61 \pm 0.035, -2.72 \pm 0.07$ ;  $17.74 \pm 0.029, -2.95 \pm 0.06$ ;  $a'_i, b_i = 14.49 \pm 0.13, -11.78 \pm 0.94$ ;  $14.36 \pm 0.12, -12.77 \pm 0.90$ ;  $\gamma_1 = 0.62 \pm 0.04, \gamma_2 = 0.010 \pm 0.01, \gamma_3^1 = 0.06 \pm 0.01, \text{ and } \gamma_3^2 = -0.01 \pm 0.01$ . This is the fit with the LMC 1993-94 data; the zero points  $\alpha'_i, a'_i$  refer to the SMC linear fits. The correction due to the metallicity dependence of the inferred distance modulus by the described technique is then  $\delta\mu = \Delta\mu_{\text{true}} - \Delta\mu_{\text{inferred}} = -0.145 \pm 0.06$  mag. If the LMC 1991-92 dataset is used, the color shift is smaller

by 0.02 *mags* to  $\gamma_3^1 - \gamma_3^2 = 0.05 \pm 0.01$ , but a corresponding change in the PL relations leads to  $\gamma_1 = 0.63 \pm 0.04$ ,  $\gamma_2 = 0.025 \pm 0.015$ ,  $\gamma_3^1 = 0.05 \pm 0.01$ , and  $\gamma_3^2 = -0.01 \pm 0.01$ . Therefore,  $\delta\mu = -0.139 \pm 0.06$  mag. In the error budget, in order of importance, the sources are: (1) the photometric transformation between the 1991-92 and present data (0.06 mag); (2) the scatter in the PL relations (0.04 mag); (3) the uncertainty in the reddening (and depth) estimate in SMC (0.03 mag). The first error source is not applicable to the LMC 1993-94 dataset.

The above result is for a fixed reddening vector,  $R_i$  (Eq. 18). If we change the parameter to  $R_V = 5.0$ , *i.e.*  $R_i = (5.51, 3.95)$ , the above result for the metallicity effect is no longer unambiguous. The reason for this is that now it is possible to satisfy the constraint from the foreground SMC reddening and correcting for the offset of the SMC Cepheids in the color-magnitude plane. In other words, if in SMC  $R_V = 5.0$  and  $E(B-V) = 0.04$ , one need not invoke a metallicity effect in the differential comparison to LMC. The fact that the SMC Cepheids appear bluer than the LMC Cepheids is then explained with the small amount of extinction and steep extinction law.

While a value of  $R_V \geq 5.0$  is not excluded (but unlikely) by our data, an extinction of  $E(B-V) = 0.04$  is very difficult to accommodate in our analysis of the magnitude residuals (see Sect. 7). Our mean value is  $0.125 \pm 0.009$ , and that is in very good agreement with a number of independent estimates, as reviewed by Bessell (1991).

Therefore we consider this alternative explanation (very high  $R_V$  and very low reddening) as very unlikely. We propose instead that the observed effect is due to the known difference in metallicity between the Cepheid samples of the LMC and SMC: 0.14 *mags* for a factor of 2 difference in heavy elements. The sign of the effect would lead to the distance of a metal-poor sample to be overestimated.

In applying the above result to other galaxies, we need to address two issues: (1) about the form of the metallicity dependence of inferred Cepheid distances, and (2) about the role of the helium abundance ( $Y$ ). The form of the dependence can be inferred from current theoretical models. Photometric colors and bolometric corrections (from model atmospheres) have linear dependencies on  $\log(\frac{Z}{0.016})$ , where  $Z$  is the abundance of metals (by mass) and  $Z = 0.016$  in the Galactic Cepheids. Mass-luminosity relations, hence  $-M_i$ , seem to depend linearly on  $Z$  (Chiosi, Wood, & Capitanio 1993; Buchler et al. 1996). In addition, these models show a significant linear dependence on the abundance of helium ( $Y$ ). We have currently no data on  $\Delta Y$  between the LMC and SMC Cepheids, therefore in applying our metallicity dependence on distance to other galaxies, we have to assume that  $(\Delta Y / \Delta Z)_{SMC-LMC} = (\Delta Y / \Delta Z)_{galaxy-LMC}$ . That assumption is strongly supported by the current level of understanding and measurement in stellar populations relevant to our study (e.g. Olive, Skillman, & Steigman 1996), and will not affect any conclusions with regards to distances. We also want to point out that the above needs to be born in mind in comparisons to results from theoretical modelling, e.g. Chiosi et al. (1993) use  $Y = 0.27$  for both LMC ( $Z = 0.008$ ) and SMC ( $Z = 0.004$ ) in Table 15, which may not be a good assumption.

In view of the above and our model, we derive the following metallicity dependence of inferred Cepheid distances:

$$\delta\mu = (0.44_{-0.2}^{+0.1}) \log \frac{Z}{Z_{LMC}}, \quad (19)$$

where  $Z$  is the abundance of metals (by mass) in the studied Cepheids and  $Z_{LMC} = 0.0085$ . The metallicity dependence is valid in the spectral region covered by the EROS filters. Due to these filters transformation properties into the standard  $BVRI$  system, and the application at hand, we have derived it for V, and V-I use in particular, where  $V - I = 1.02(B_E - R_E)$ ,  $\sigma = 0.02$  *mags*. The above metallicity dependence applies to distances inferred by differencing against the LMC Cepheids and Cepheid derived reddenings (what we refer to as the *modern technique*), and  $R_V(LMC) = 3.3$ .

The metallicity dependence we find is two times less steep than that found by Gould (1994) from Freedman & Madore's M31 data ( $0.88 \pm 0.16$  [Fe/H]). It is also smaller than Stothers' prediction ( $28.7 \delta Z$ , for  $\delta Y / \delta Z = 3.5$ ). However our result is in perfect agreement with the metallicity effect seen in Galactic Cepheids as a function of galactocentric distance. The observed abundance gradient for Cepheids is  $\delta[Fe/H] / \delta R_{GC} = -0.07 \pm 0.02 \text{ kpc}^{-1}$  (Giridhar 1986). Two independent Cepheid samples show the same effect of progressively bluer color with increasing galactocentric distance (Caldwell & Coulson 1987, and Gieren et al. 1993), which converts to the following values for  $\gamma_3^1 - \gamma_3^2$  (of Eq. 10) in units of [Fe/H]:  $0.29 \pm 0.05$  for (B-V), and  $0.20 \pm 0.05$  for (V-I). For (V-I) of our system we obtained  $0.20 \pm 0.02$ . Exactly the same value is obtained (and a nice illustration of the effect) from the compilation of LMC and SMC Cepheids in the study by Di Benedetto (1995) – see his Fig. 1 & 2, and also 8.

Our comparison to the work of Caldwell & Coulson (1986) in  $BVI$  and of Laney & Stobie (1994) in  $VJHK$  is limited for at least two reasons. First, we cannot reproduce their reddening determinations with only two bands. Second, we are unable to comment on the theoretical models which they used as constraints. Nevertheless, we find a similar intrinsic difference in  $V - I$  colors between LMC and SMC as Caldwell & Coulson; our value is two times larger. We also agree with Laney & Stobie's main conclusions, despite the uncertainty of a  $J$  to  $I$  transformation needed for such a comparison.

The metallicity dependence is not strong enough to upset the overall agreement of the four primary distance indicators in fifteen local distances (Huterer, Sasselov, & Schechter 1995). Similarly, the discrepant distance moduli involving IC 1613 noted by Gould (1994) are less discrepant with our weaker metallicity dependence; the RR Lyrae distances may be partly responsible for the remaining difference.

## 8.2. Implications for $H_0$

Despite its relative weakness, this metallicity dependence has a significant effect on extragalactic distance measurements. The effect of metallicity on Cepheid luminosity, when not accounted for, can lead to two types of errors in distance measurements

(Gould 1994): incorrect  $H_0$  value, or a dependence of  $H_0$  on distance appearing as proper motions or Malmquist bias. Here we illustrate the effect of our metallicity dependence on the value of  $H_0$ , as based on Cepheids.

Recent efforts to determine  $H_0$  from Cepheid distances have focused on: (1) the Virgo and Fornax cluster galaxies (Freedman et al. 1994b, 1996), (2) the Leo I group, containing ellipticals (Tanvir et al. 1995); and (3) the parent galaxies of supernovae of type Ia (Sandage et al. 1994). All these studies use the same modern technique with the LMC as a base and all the same initial assumptions; we share them in our analysis. Yet they result in three different values of  $H_0$ , with hardly overlapping error bars. The abundances of metals in the young populations of the host galaxies for these studies differ and, apparently, in a systematic way. Therefore we propose that the metallicity dependence may be responsible for most of this discrepancy. To illustrate our idea, below we apply Eq. (19); please note that the uncertainties in the metallicities of the extragalactic Cepheids are not yet well known, hence we do not try to provide rigorous error estimates to the corrected values.

With the first approach and HST  $VI$  photometry of Cepheids in M100, Freedman et al. (1994b) derive  $H_0 = 80 \pm 17 \text{ km.s}^{-1} \text{ Mpc}^{-1}$ . For the metallicity of the Cepheids we adopt  $[\text{Fe}/\text{H}] = +0.1$  ( $Z=0.021$ ), derived from the abundances of H II regions (Zaritsky et al. 1994), assuming a solar  $[\text{O}/\text{Fe}]$  ratio. With the uncertainty range for the slope of our metallicity effect, this leads to  $H_0 = 76 - 70 \text{ km.s}^{-1} \text{ Mpc}^{-1}$ . With some of the color difference due to metallicity effects, the estimate of interstellar reddening will also change (the metal-rich M100 Cepheids are intrinsically “redder” than the LMC ones) – e.g. from  $E(V-I) = 0.13 \pm 0.06$  (after Ferrarese et al. 1996) we obtain  $0.05 \text{ mags}$ . Recent interim results reported on half-dozen more galaxies (Freedman, Madore, & Kennicutt 1996) include mostly spirals which are not as metal rich as M100, e.g. M101 has LMC abundances in its outer field. All this brings their interim result down to  $73 \pm 10$  from their initial M100-based value, as we would expect from our metallicity effect. A complete analysis should be done when all data becomes available.

With the second approach and HST  $VI$  photometry of Cepheids in M96, Tanvir et al. (1995) derive  $H_0 = 69 \pm 8 \text{ km.s}^{-1} \text{ Mpc}^{-1}$ . The abundance estimate for M96 comes from Oey & Kennicutt (1993), slightly below solar at  $[\text{Fe}/\text{H}] = -0.02$ . This implies a small change in the Cepheid distance to M96 and a decrease in the value of  $H_0$  by  $3-5 \text{ km.s}^{-1} \text{ Mpc}^{-1}$ . The reddening changes from  $E(V-I) = 0.09 \pm 0.10$  to  $0.03 \text{ mags}$ .

With the third approach and HST  $VI$  photometry of Cepheids in IC4182 and NGC5253, Sandage et al. (1994) derive  $H_0 = 55 \pm 8 \text{ km.s}^{-1} \text{ Mpc}^{-1}$ . Abundances in NGC5253 have been measured and discussed by Pagel et al. (1992); discussion of abundances in IC4182 is given by Saha et al. (1994) – we adopt  $[\text{Fe}/\text{H}] = -1.3$  and caution on the large uncertainties. With this metallicity the above estimate of  $H_0$  should be increased by 6 to  $13 \text{ km.s}^{-1} \text{ Mpc}^{-1}$ . The reddening estimates change from  $E(V-I) = -0.11 \pm 0.07$  and  $0.03 \pm 0.15$ , to  $E(V-I) = 0.09 \pm 0.07$  and  $0.23 \pm 0.15$ , respectively (these metal-poor Cepheids are “bluer” than the LMC ones). Here we should

point out that the interpretation of the light curves of SN Ia themselves has been improved considerably by Riess, Press, & Kirshner (1995), leading to an additional systematic shift upwards by  $6 \text{ km.s}^{-1} \text{ Mpc}^{-1}$ . This brings about the estimate to  $H_0 \approx 70$ , which is also in good agreement with the theoretical calibration of SN Ia and the value  $H_0 = 67 \pm 9 \text{ km.s}^{-1} \text{ Mpc}^{-1}$  by Höflich & Khokhlov (1996). The new value of  $H_0 = 58 \pm 4 \text{ km.s}^{-1} \text{ Mpc}^{-1}$  by Sandage et al. (1996) includes two SNe Ia in spiral galaxies, in which Cepheid metallicity is most likely similar to that of the LMC. Note, however, that the two SNe – 1981B (NGC4536) and 1990N (NGC4639) are by  $0.2-0.4 \text{ mags}$  dimmer than the three SNs in IC4182 and NGC5253. Therefore, the result we obtained above by accounting the effect of metallicity on the Cepheid distances for each galaxy, remains virtually unchanged, and so does the consistency with the results of Riess, Press, & Kirshner (1995).

The metallicity dependence we found from the LMC/SMC analysis brings all the derivations of  $H_0$  to good agreement. It also leads to reasonable amounts of reddening, especially regarding the negative values obtained otherwise in metal-poor samples.

Secondary distance indicators, like the Tully-Fisher (TF) relation, the Surface Brightness Fluctuations (SBF) method, and the Planetary Nebulae Luminosity Function (PNLF) method, have their zero points calibrated with Cepheids. The TF relation is calibrated primarily in M81 (Freedman et al. 1994a) with 25 Cepheids. The metallicity of these Cepheids is high,  $[\text{Fe}/\text{H}] \approx 0.05$  (Garnett & Shields 1987; Zaritsky et al. 1994). The SBF and PNLF zero points come from M31, and in a similar fashion – from metal-rich Cepheids (Freedman & Madore 1990). Given our metallicity effect, we are not surprised to note that all these methods give a high value for  $H_0$ .

## 9. Conclusions

We use the new EROS microlensing survey data-set of 3 million two-color observations of about 500 Cepheids in the LMC and SMC to search for and derive the dependence of the optical PL relations on metallicity. We find that:

- (1) The PL relations for both types of Cepheids have the same zero-point offset (but no slope difference), which is attributed to the effect of metallicity under a reasonable assumption about the extinction law. As expected from theory, this effect of metal content is manifested in a color shift of the instability strip. It amounts to about  $\frac{1}{3}$ th of the strip width, and we could detect it unambiguously thanks to the large number of Cepheids and extremely well sampled light curves.
- (2) With the known ensemble difference in metal content between LMC and SMC Cepheids, we derive a linear relation between the distance modulus correction and metallicity:

$$\delta\mu = (0.44_{-0.2}^{+0.1}) \log \frac{Z}{Z_{LMC}},$$

It applies to distances which are inferred by using LMC as a base and using two color  $VI$  photometry of the Cepheids to establish the reddening. The linearity of metallicity dependence is a good

assumption, but needs to be confirmed empirically outside the range of application (a factor of few lower than SMC and higher than the Galaxy).

(3) The first overtone Cepheids have PL relations which provide distances fully consistent with the PL relations of fundamental mode Cepheids .

We use two color bands closely spaced in wavelength because of availability, not their desirability; ideally one would like to use at least three bands, one of them in the near-infrared.

Our result can be applied to the long-standing discrepancy between the low- $H_0$  scale and the high- $H_0$  scale. The host galaxies on which each of these scales relies appear to have systematically different metallicities. A simple application of our correction to several recent derivations makes the low- $H_0$  values (Sandage et al. 1994) *higher* and the high- $H_0$  values (Freedman et al. 1994b) *lower*, thus bringing those discrepant estimates into agreement near  $H_0 \sim 70 \text{ km.s}^{-1} \text{ Mpc}^{-1}$ .

*Acknowledgements.* We are grateful for the support given to our project by the technical staff at ESO La Silla and thank D. Welch for his helpful suggestions.

## References

- Alcock C., Akerlof C.W., Allsman R.A., Axelrod T.S., Bennett D.P., Chan S., Cook K.H., Freeman K.C., Griest K., Marshall S.L., Park H-S., Perlmutter S., Peterson B.A., Pratt M.R., Quinn P.J., Rodgers A.W., Stubbs C.W., Sutherland W. *Nature*, 1993, **365**, 621
- Aubourg E., Baryre P., Brehin S., Gros M., Lachieze-Rey M., Laurent B., Lesquoy E., Magneville C., Milsztajn A., Moscoso L., Queinnec F., Rich J., Spiro M., Vigroux L., Zylberajch S., Ansari R., Cavalier F., Moniez M., Beaulieu J.P., Ferlet R., Grison Ph., Vidal-Madjar A., Guibert J., Moreau O., Tajahmady F., Maurice E., Prevot L., Gry C., *The Messenger*, 1993a, **72**, 20
- Aubourg E., Baryre P., Brehin S., Gros M., Lachieze-Rey M., Laurent B., Lesquoy E., Magneville C., Milsztajn A., Moscoso L., Queinnec F., Rich J., Spiro M., Vigroux L., Zylberajch S., Ansari R., Cavalier F., Moniez M., Beaulieu J.P., Ferlet R., Grison Ph., Vidal-Madjar A., Guibert J., Moreau O., Tajahmady F., Maurice E., Prevot L., Gry C., *Nature*, 1993b, **365**, 623
- Beaulieu, J.P., et al. 1996, in preparation.
- Bessell, M.S. 1991, *A&A*, 242, L17
- Buchler, J.R., Kollath, Z., Beaulieu, J.P., & Goupil, M.J., 1996, *ApJL*, 462, L83.
- Caldwell, J.A.R. & Coulson, I.M., 1985, *MNRAS*, 212, 879
- Caldwell, J.A.R. & Coulson, I.M., 1985, *MNRAS*, 218, 223
- Caldwell, J.A.R. & Coulson, I.M., 1987, *AJ*, 93, 1090
- Chiosi, C., Wood, P.R., & Capitanio, N., 1993, *ApJS*, 86, 541.
- Di Benedetto, G.P., 1995, *ApJ*, 452, 195.
- Feast, M.W. 1991, in *Observational Tests of Cosmological Inflation*, eds. Shanks et al., p.147.
- Feast, M.W. 1995, in *Astrophysical Applications of Stellar Pulsation*, eds. Stobie & Whitelock, ASP (San Francisco), p.209.
- Ferrarese, L., Freedman, W.L., Hill, R.J., Saha, A., et al. 1996, *ApJ*, 464, 568
- Freedman, W.L., & Madore B.F., 1990, *ApJ*, 365, 186
- Freedman, W.L., Hughes, S. M., Madore, B.F., et al. 1994a, *ApJ*, 427, 628
- Freedman, W.L., Madore, B.F., Mould, J. R., et al. 1994b, *Nature*, 371, 757
- Freedman, W.L., Madore, B.F., & Kennicutt, R.C. 1996, in *STScI Symposium on "The Extragalactic Distance Scale"*, ed. M.Livio, in press.
- Gieren, W.P., Barnes, T.G., & Moffett, T.J. 1993, *ApJ*, 418, 135
- Giridhar, S. 1986, *J.Astrophys.Astron.*, 7, 83
- Gould, A. 1994, *ApJ*, 426, 542
- Höfllich, P. & Khokhlov, A. 1996, *ApJ*, 458, 500
- Huterer, D., Sasselov, D.D., & Schechter, P.L. 1995, *AJ*, 110, 2705
- Laney, C.D., & Stobie, R.S. 1994, *MNRAS*, 266, 441.
- Madore, B.F., & Freedman, W.L. 1991, *PASP*, 103, 933
- Martin, W.L., Warren, P.R., & Feast, M.W. 1979, *MNRAS*, 188, 139.
- Oey, M.S., & Kennicutt, R.C. 1993, *ApJ*, 411, 137
- Olive, K.A., Skillman, E., & Steigman, G., 1996, preprint (UMN-TH-1514/96), astro-ph/9611166.
- Pagel, B.E.J., Simonson, E.A., Terlevich, R.J., & Edmunds, M.G. 1992, *MNRAS*, 255, 325
- Pierce, M.J., Welch, D.L., McClure, R.D., van den Bergh, S., Racine, R., & Stetson, P.B. 1994, *Nature*, 371, 385
- Press, W.H., Teukolsky, S.A., Vetterling, W.T., & Flannery, B.P. 1992, *Numerical Recipes*, 2nd Ed., (Cambridge University Press, Cambridge)
- Press, W.H. 1996, preprint, astro-ph/9604126.
- Riess, A.G., Press, W.H., & Kirshner, R.P. 1995, *ApJ*, 438, L17
- Saha, A., Labhardt, L., Schwengeler, H., Macchetto, F.D., Panagia, N., Sandage, A., & Tammann, G.A. 1994, *ApJ*, 425, 14
- Sandage, A., Saha, A., Tammann, G.A., Labhardt, L., Schwengeler, H., Panagia, N., & Macchetto, F.D. 1994, *ApJ* **423**, L13
- Sandage, A., Saha, A., Tammann, G.A., Labhardt, L., Panagia, N., & Macchetto, F.D. 1996, *ApJL*, in press.
- Schechter, P.L. 1980, *AJ*, 85, 801
- Stift, M.J. 1982, *A&A*, 112, 149
- Stift, M.J. 1995, *A&A*, 301, 776
- Stothers, R. B. 1988, *ApJ*, 329, 712
- Tanvir, N.R., Shanks, T., Freguson, H.C., & Robinson, D.R.T. 1995, *Nature*, 377, 27
- Zaritsky, D., Kennicutt, R.C., & Huchra, J. P. 1994, *ApJ*, 420, 87